

Combining Power Electronic Converters and Automation to Simulate Solar PV systems

Armando Cordeiro

Department of Electrical Engineering
and Automation ; LCEC, DEEEA ;
ISEL, Instituto Politécnico de Lisboa ;
INESC-ID
Lisbon, Portugal
armando.cordeiro@isiel.pt

Filipe Barata

Department of Electrical Engineering
and Automation
ISEL, Instituto Politécnico de Lisboa
Lisbon, Portugal
filipe.barata@isiel.pt

V. Fernão Pires

INESC-ID
SustainRD
ESTSetúbal, Polytechnic Institute of
Setúbal
Setúbal, Portugal
vitor.pires@estsetubal.ips.pt

Miguel Chaves

Department of Electrical Engineering
and Automation
ISEL, Instituto Politécnico de Lisboa ;
INESC-ID
Lisbon, Portugal
miguel.chaves@isiel.pt

Pedro Fonte

Department of Electrical Engineering
and Automation ; LCEC, DEEEA
ISEL, Instituto Politécnico de Lisboa
Lisbon, Portugal
pedro.fonte@isiel.pt

Daniel Foito

SustainRD
ESTSetúbal, Polytechnic Institute of
Setúbal, Setúbal, Portugal
CTS – Uninova
Lisbon, Portugal
daniel.foito@estsetubal.ips.pt

J. F. Martins

CTS – Uninova
DEEC/FCT/UNL
Lisbon, Portugal
jf.martins@fct.unl.pt

Paulo Gâmbao

Department of Electrical Engineering
and Automation
ISEL, Instituto Politécnico de Lisboa ;
INESC-ID
Lisbon, Portugal
paulo.gambao@isiel.pt

Hélio Lopes

Department of Electrical Engineering
and Automation
ISEL, Instituto Politécnico de Lisboa
Lisbon, Portugal
A35328@alunos.isiel.pt

Tito Amaral

SustainRD
ESTSetúbal, Polytechnic Institute of
Setúbal
Setúbal, Portugal
tito.amaral@estsetubal.ips.pt

Abstract— This paper presents a solar photovoltaic panel simulator system with the ability to perform automatic tests in different condition according to manufacture parameters. This simulator is based on three buck-boost DC-DC converters controlled by a microcontroller and supported by a Programmable Logic Controller which is responsible for the automatic tests. This solution will allow to achieve fast response, like suddenly changes in the irradiation, temperature, or load. To control the power converter, it will be used a fast and robust sliding mode controller. Therefore, with the proposed system is possible to perform the I-V curve simulation of a solar PV panel, evaluate different MPPT algorithms considering different meteorological and load variation. The main advantage of this work is the possibility to evaluate and test several MPPT algorithms and understand the operation and typical operation of solar PV panels in different conditions. Several simulations and experimental results from a laboratory prototype are presented to confirm the theoretical operation.

Keywords— PV simulator; Emulator; PV system; Sliding mode controller; Buck-Boost DC-DC converter; PLC.

I. INTRODUCTION

The use of renewable energies, especially through solar photovoltaic (PV) panels is increasingly widespread in all parts of the world. Investments in renewable power capacity have been increasing over the last years, and electrical production/distribution corporations are continuously breaking records for sourcing renewable electricity. Also, more and more countries are turning towards electrification with renewables. According to the latest report from REN21 [1], an estimated 256 gigawatts (GW) of renewable power capacity were added globally during the year of 2020, surpassing the previous record by nearly 30%. Solar PV had another record-breaking year in 2020, with new installations

reaching an estimated 139 GWDC (GigaWatt Direct Current) and the global total solar PV is estimated around 760 GWDC, including both on-grid and off-grid capacity.

These numbers reveal that solar PV play an important role in the present global electricity generation due to supporting government policies, climate change awareness and benefits from technological advances (with solar cell efficiencies increasing steadily), and lower production costs due to massive production driven by the growth of new markets. Nevertheless, there are still issues to be investigated and improved in the design of components of PV systems. There are also other aspects related to learning of the operation, control and test the solar PV systems to easily integrate them in both on-grid and off-grid applications. To continue promoting the development and installation of solar panels, it is also necessary to invest in the training of technicians and young researchers.

The main difficulty during the testing of PV panels is related about the unpredictability of the operating conditions; temperature and irradiation are not consistent over the day and the relative position between the sun and the panel is constantly changing. Besides that, field tests are usually very expensive and depends strongly on meteorological conditions. To address this difficulty several methods of solar PV simulators with different strategies can be found in literature. Some authors have dedicated the investigation to PV simulators regarding recording of operational data for reliability analysis [2], others are dedicated to theoretical simulation models, such as one-diode equivalent circuit model [3], dual-diode model [4], seven-parameter model [5], end-to-end differentiable power [6], or voltage temperature simulation algorithms [7]. Other authors suggested solutions using constant voltage DC power supply and variable

resistances [8]. A PV panel simulator based on a nonlinear power source for high power application is suggested in [9]. Some alternative solutions based on switch-mode power converters have also been proposed [10-14]. Similar low-cost microcontroller-based solutions using Buck, Boost or Buck-Boost DC-DC converters can be found in [15-18]. Some of the mentioned solutions are not flexible to change in case of different PV module types or are not able to redefine the operation conditions such as solar irradiance and/or temperature. Others are not able to define and select different MPPT (maximum power point tracker) algorithms.

In this paper it is proposed a solar PV panel simulator system up to 350W based on three buck-boost DC-DC power converters with a sliding mode controller capable to reproduce the necessary simulation and test conditions automatically. The core of this solar PV panel simulator system is based on a microcontroller supported by a PLC (Programmable Logic Controller), making possible to evaluate the performance of different MPPT algorithms, solar PV panels, solar irradiation, temperature, and load variation. As a result, due to the adopted power converter topology and the proposed automated controlled system, it is obtained a solution that allows a fast change in the simulator control system according to necessary modifications, achieving a good performance in different conditions and with different MPPT algorithms. The main novelty of this work is the possibility to test automatically the I-V curves of different PV panels according with data available from manufacture manuals. Additionally, it is also novelty the possibility to test automatically different MPPT algorithms in order to evaluate their performance. Besides this introduction, in section II will be presented the description of the proposed PV panel simulator. Section III is dedicated to the adopted model of the PV panel and section IV to the control system of the converter which simulates the I-V characteristic curves. The simulation results will be presented in section V and the experimental results in section VI. Finally, the conclusions are presented in section VII.

II. SYSTEM DESCRIPTION

The proposed solution is composed by a DC power source, three classic buck-boost DC-DC converters, a DSP microcontroller, a PLC combined with a SCADA (Supervisory Control and Data Acquisition) software, two signal conditioning boards (voltage and current), one PWM modulator circuit, two analog sliding mode circuits and a RL load. The solution is able to operate in two different modes, namely the test panel mode (mode I) and the MPPT test mode (Mode II). The block diagram of the mode I can be seen in Fig.1. This mode is dedicated to test and simulate the I-V curve of the panel according to data parameters of the manufacture considering different solar irradiance and temperature reference values. In this mode only two DC-DC buck-boost converters are used (only in buck operation; the first simulates the solar PV panel; the second to perform the load variation through Pulse Width Modulation - PWM). The first step consists in adjusting the DC power source to 60V. The second step consists in introducing the solar panel parameters, desired solar irradiance, and temperature reference values within the SCADA software. In this software is possible to define up to 24 reference values for irradiance and local temperature and up to 12 variable load percentage values. After completed this operation, the SCADA software sends all the information to the PLC which is responsible to

send the desired data to the DSP microcontroller through the RS232C communication channel. After receiving all the information, the PLC runs the program to automate the simulation tests and starts the operation of the DSP device to simulate the solar PV panel I-V curve. The PLC program changes the pre-specified reference values for irradiance and local temperature at each 20 second and records the solar PV voltage and current feedback in the PLC memory registers. After finishing the simulation tests for all the pre-specified reference values, the results are displayed in the SCADA screen layout to the operator. The communication between the SCADA software and the PLC is performed using the Modbus TCP/IP protocol.

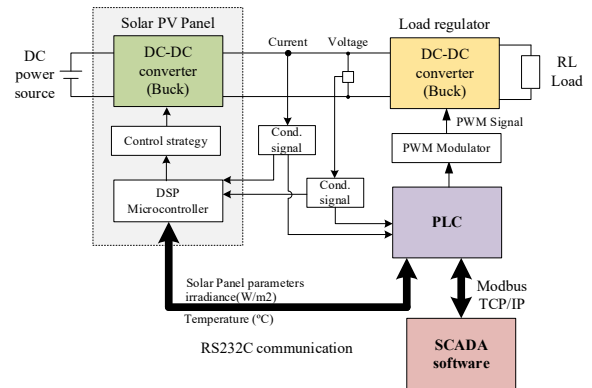


Fig. 1. The block diagram of the mode I (test panel mode).

The block diagram of mode II can be seen in Fig.2. This solution is used to perform a test to the MPPT control algorithm and evaluate the delivered power in different load conditions. In this mode the three DC-DC buck-boost converters are used, where two of them operate in buck mode and the other in boost mode (see Fig.2). The operation is similar to mode I but in this mode the user also selects the desired MPPT algorithm in addition to all the other parameters. In the proposed solution only two classical MPPT techniques [19], [20] were implemented, namely the perturb and observe (P&O) and the hill climbing (HC). Other classic MPPT techniques such as the improved P&O, constant voltage (CV), incremental conductance (InC), open-circuit voltage (OCV), short-circuit current (SCC) or the adaptive reference voltage (ARV) can be implemented if desired. These techniques are easily implemented because of their less complexity in the algorithm and are most efficient for uniform irradiation conditions as the PV will generate only one Global MPP in these conditions.

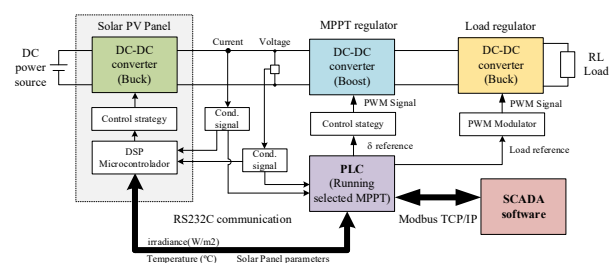


Fig. 2. The block diagram of the mode II (MPPT test mode).

Nevertheless, these algorithms have rapid oscillations around the MPP, which results in the loss of power [21]. Other intelligent or hybrid MPPT techniques are more complex and require fast processing devices which are not compatible with the speed of most PLCs.

To avoid the development of different converters in the proposed solution, it was adopted a single PCB board type with the classic buck-boost DC-DC converter. Connecting the converter from the left to the right (switching S2 and maintaining S1 turned off) operates as boost topology. In the opposite direction operates as buck topology (switching S1 and maintaining S2 turned off). Fig. 3 illustrates the classic buck-boost DC-DC converter adopted.

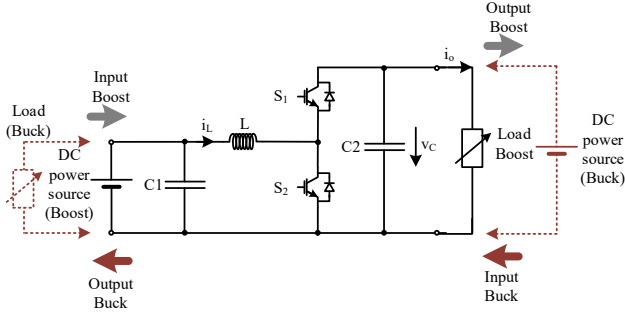


Fig. 3. Classic buck-boost DC-DC topology adopted.

III. SOLAR PV PANEL MODEL

The proposed solar PV simulator is composed by a buck-boost DC-DC converter operating in buck mode. In order to obtain a fast response, a sliding mode controller is adopted as will be explained in the next section. The solar PV simulator is controller in order to emulate the output PV panel voltage at the terminals of the capacitor C1 (see Fig.3). Thus, the reference of the controller must be generated by an I-V characteristic of PV module that is in test according to manufacture parameters. The adopted solar PV panel model is one of the most used and adopted by industry, the single diode model [22]. The equivalent circuit of this model is presented in Fig. 4.

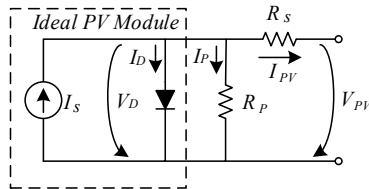


Fig. 4. Electric equivalent circuit of a PV module using the single diode model.

In this model I_{PV} is the output current of the cell module; I_S indicates the ideal photocurrent due to the module cell surface temperature T_S and solar irradiation G ; I_D is the diode current; I_P is the current flowing through an internal parallel resistor caused by an imperfect P-N junction; the internal parallel and series equivalent resistances are represented by R_P and R_S respectively. From the analysis of the circuit by the Kirchoff laws, the following relationship between the currents can be obtained by (1).

$$I_{PV} = I_S - I_D - I_P \quad (1)$$

The I_S photocurrent is given by (2).

$$I_S = \frac{[I_{SC} + k_i(T_S - T)]G}{1000} \quad (2)$$

Where I_{SC} is the equivalent short-circuit current at the irradiation reference $G=1000W/m^2$ and temperature reference of $T=298.15K$ ($\approx 25^\circ C$); k_i is the temperature modification coefficient for the equivalent short-circuit current. In this model, the diode represents the P-N junction and its (dark) current I_D (3) which is dependent of the output voltage V_{PV} , output current I_{PV} , elementary electron charge $q=1.6022 \times 10^{-19} C$, n as the ideality factor (usually this value is between 1 and 5), Boltzmann constant $K=1.3806 \times 10^{-23} J/K$ and the reference temperature which is $T=298.15K$ ($\approx 25^\circ C$).

In (3), I_O represents the reverse saturation current.

$$I_D = I_O \left(\exp \left(q \frac{V_{PV} + I_{PV} R_S}{nKT} \right) - 1 \right) \quad (3)$$

The current I_P flowing through the internal parallel resistance is given by (4).

$$I_P = \frac{V_D}{R_P} = \frac{V_{PV} + (R_S I_{PV})}{R_P} \quad (4)$$

The reverse saturation current I_O is given by (5).

$$I_O = I_{rr} \left(\frac{T_S}{T} \right)^3 \exp \left[\frac{qE_g}{nK} \left(\frac{1}{T} - \frac{1}{T_S} \right) \right] \quad (5)$$

Where I_{rr} represents reverse saturation current at $T=25^\circ C$ and $E_g \approx 1.1eV$ is the energy gap for an Si semiconductor. This current is dependent on the module cell surface temperature T_S . The combination of (1) to (4) leads us to the I-V characteristic (6) for a unique cell module.

$$I_{PV} = I_S - I_O \left(\exp \left(\frac{(V_{PV} + R_S I_{PV}) q}{nKT} \right) - 1 \right) - \frac{(V_{PV} + R_S I_{PV})}{R_P} \quad (6)$$

In short-circuit conditions, the output voltage is zero and both I_D and I_P ($R_P \gg R_S$) currents can be neglected, so the output current presents its maximum value:

$$I_{PV_SC} \approx I_S \quad (7)$$

On the other hand, for open-circuit conditions, the output current is effectively zero, so the output voltage presents its maximum value:

$$V_{PV_OC} = \frac{nKT}{q} \left[1 + \ln \left(\frac{I_{SC} - I_P}{I_O} \right) \right] \quad (8)$$

The influence of solar irradiation and temperature in the open-circuit voltage and short-circuit current are given by (9) and (10), where V_{OC_STC} and I_{SC_STC} are the open-circuit voltage and short-circuit current under standard test conditions (STC) respectively; k_V and k_i are the voltage and current modification coefficient temperature coefficients, respectively. The values of V_{OC_STC} , I_{SC_STC} , k_V and k_i are specified by the solar PV module manufacture.

$$V_{PV_OC} = \frac{(V_{OC_STC} + k_V \cdot (T_S - 298,15))G}{1000} \quad (9)$$

$$I_{PV_SC} = \frac{(I_{SC_STC} + k_i(T_S - 298,15))G}{1000} \quad (10)$$

IV. CONTROL OF THE SOLAR PV PANEL SIMULATOR

As explained in the previous section, the power converter which generates the I-V curve will be controlled by a sliding mode controller. The control of the power converter associated with the MPPT can be performed using a similar strategy. The dynamics of this controller presents a fast response and robustness to load and parameter variation [23], [24]. Due to these features, it has been used in several applications [25], [26]. To design this controller, it will be used a dynamic model where it is supposed zero losses in the capacitors, inductors, and power semiconductors. The state of the power device S1 can be represented by the time dependent variable γ , which is defined as:

$$\gamma = \begin{cases} 1, S1 \rightarrow ON \\ 0, S1 \rightarrow OFF \end{cases} \quad (11)$$

Analyzing the circuit presented in Fig. 3 (considering the time dependent variable) the following simplified switched state-space model of the power converter is obtained by (12).

$$\begin{cases} \frac{di_L}{dt} = -\frac{1}{L}v_{C1} + \frac{\gamma}{L}v_{DC} \\ \frac{dv_{C1}}{dt} = \frac{1}{C1}i_L - \frac{1}{C1}i_o \end{cases} \quad (12)$$

Considering the dynamics of (12), it is possible to obtain the equation for the output voltage controller considering the associations between currents and voltages. Taking into consideration the v_{C1} capacitor voltage as the controlled output, based on (12) the state-space equations in the controllability canonical form can be obtained by (13) and (14). Notice that i_o is the output current on the left side of Fig.3 (buck operation), which is equivalent to I_{PV} .

$$\lambda = \frac{i_L - i_o}{C1} \quad (13)$$

$$\frac{d}{dt} \begin{bmatrix} v_{C1} \\ \lambda \end{bmatrix} = \begin{bmatrix} \lambda \\ -\frac{1}{LC1}v_{C1} - \frac{1}{C1}\frac{di_o}{dt} + \frac{\gamma}{LC1}v_{DC} \end{bmatrix} \quad (14)$$

From these new state-space equations, it is possible to analyze that the output current has a strong relative degree of two [23] (since only its second time derivative contains the control variable). Therefore, it can be concluded that the sliding surface defined in (15) ensures the robustness and stability of the closed loop system as presented in [24].

$$S(e_{v_{C1}}, e_{\lambda}) = (v_{C1ref} - v_{C1}) + \beta(\lambda_{ref} - \lambda) \quad (15)$$

Where β is the parameter related with the time constant of the desired first order response of the input source current ($\beta > 0$). Based on (13) and (15) is possible to define the sliding surface as presented in (16).

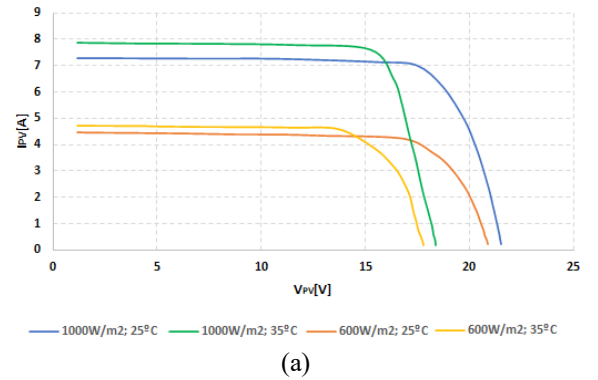
$$S(e_{v_{C1}}, e_{\lambda}) = (v_{C1ref} - v_{C1}) + \beta \frac{dv_{C1ref}}{dt} - \frac{\beta}{C1}(i_L - i_o) \quad (16)$$

Nevertheless, considering that in practical applications the power semiconductors present a limited switching frequency, it is necessary to impose a limited bandwidth to the pulse drive of the power semiconductors. To solve this issue is necessary to use a hysteresis comparator, in order to maintain the sliding surface near zero with limited switching frequency. Therefore, the control law for the power semiconductor S1 is chosen as described in (17), where Δ is an arbitrary small quantity that imposes the desired limited bandwidth.

$$\begin{cases} \text{if } S(e_{v_c}, e_{\theta}) > \Delta \text{ or} \\ \left[\dot{S}(e_{v_c}, e_{\theta}) < 0 \text{ and } |S(e_{v_c}, e_{\theta})| < \Delta \right] \text{ then } S_1 = ON; \\ \text{if } S(e_{v_c}, e_{\theta}) < -\Delta \text{ or} \\ \left[\dot{S}(e_{v_c}, e_{\theta}) > 0 \text{ and } |S(e_{v_c}, e_{\theta})| < \Delta \right] \text{ then } S_1 = OFF; \end{cases} \quad (17)$$

V. SIMULATION TESTS

The proposed solution was simulated using the MATLAB/Simulink software. For the simulation of the solar PV array, it was chosen the ideal model described in section III. The data for this model was obtained from the commercial PV SGP-120W18V Poly Solar Panel [27]. The values selected for the passive components of all the DC-DC converters were $L = 1\text{mH}$, $C1 = C2 = 470\mu\text{F}$. The DC power source was adjusted to $60V_{DC}$. The first simulation test was created in mode I (test panel mode) in order to evaluate the I-V characteristic curves of the solar PV panel considering the different solar irradiations and temperatures. The simulation results presented in Fig.5 show the I-V and P-V curves in four different situations: (1)– $G=1000\text{W/m}^2$, $T=25^\circ\text{C}$; (2)– $G=600\text{W/m}^2$, $T=25^\circ\text{C}$; (3)– $G=1000\text{W/m}^2$, $T=35^\circ\text{C}$; (4)– $G=600\text{W/m}^2$, $T=35^\circ\text{C}$.



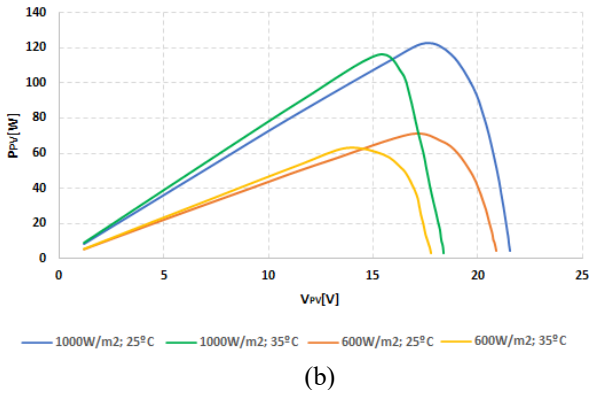


Fig. 5. Simulation results for the parameters of the solar PV SGP-120W18V [27]: (a) I-V and (b) P-V characteristic curves.

The second simulation test was created in mode II (MPPT test mode) to evaluate the dynamic operation of the MPPT algorithm. The MPPT algorithm selected was the perturb and observe (P&O). The result of this test is presented in Fig. 6. In this simulation result is possible to see that despite the load variation (at 0.25s, 0.5s and 0.75s), after the disturbances, the system delivers to the load the same output power, thanks to the MPPT algorithm executed by the second DC-DC converter operating in boost mode. Notice that the waveforms presented in Fig. 6 represent the output values of the boost converter.

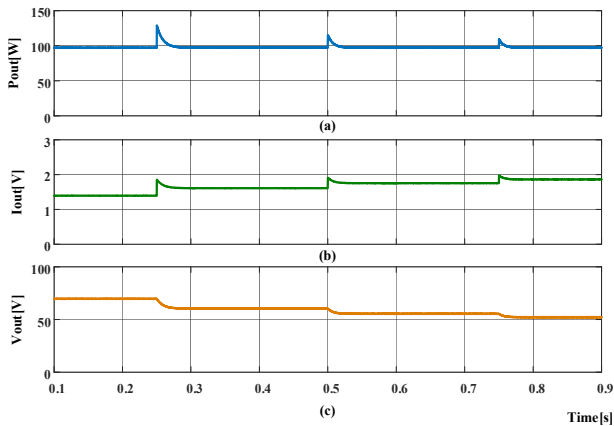


Fig. 6. Simulation results considering the system operating in mode II (MPPT test mode): (a) Output power, (b) output current and (c) output voltage of the boost converter controlled using the perturb and observe (P&O) MPPT algorithm.

VI. EXPERIMENTAL TESTS

In this section several experimental results are presented to demonstrate the operation of the proposed simulation and test system. The experimental results were obtained using the laboratorial setup presented in Fig. 7. In this figure is possible see the three DC-DC converters (green PCBs which include two C2M0080120D SiC MOSFET and the respective drive circuits) with the respective inductors, a PLC (Phoenix Contact), a red PCB with current sensors, a yellow PCB with voltage sensors, and the Microchip DSP microcontroller mounted in a breadboard circuit. To supply the system, it was used a laboratorial DC power source adjusted to 60V. The passive components of the DC-DC converters are like those selected in the simulation tests described in the previous section.

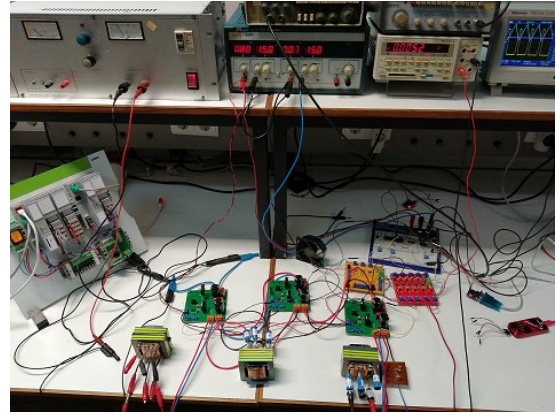


Fig. 7. Experimental setup of the proposed system

The first experimental test was performed to evaluate the operation of the buck DC-DC converter associated to the solar PV simulator and the DSP microcontroller performance to accomplish the I-V characteristic curves (mode I). The result of the first test can be seen in Fig. 8, showing the current (Ch1-1A/div) and voltage (Ch3-5V/div) considering a continuous load variation and a solar irradiation change from 600W/m² to 1000W/m² at 25°C.

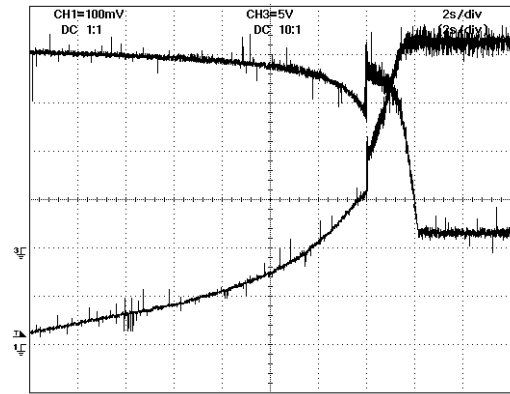


Fig. 8. Experimental result in mode I (test panel mode). Output current (CH1) and output voltage (CH3) considering a step solar irradiation from 600 W/m² to 1000 W/m² both at 25 °C.

The results presented in Fig.9 shows a comparison between the simulation and experimental (average values) results regarding the I-V characteristic curves obtained in both situations. These results show similar curves which indicate the validation of the solar PV panel model parameters and control strategy adopted.

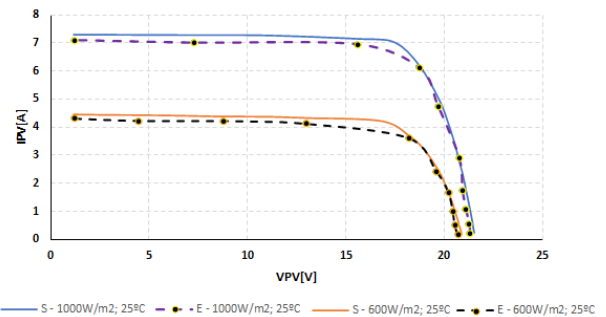


Fig. 9. Comparison of simulation and experimental results regarding the I-V characteristic curves of the solar PV SGP-120W18V [27].

Another experimental result is presented in Fig.10. In this case the test was performed in mode II (MPPT test mode). The MPPT algorithm was designed to continually control the

duty-cycle of the boost DC-DC converter. This result shows the output power (Ch3), current (Ch2-1A/div) and voltage (Ch1-50/div) of the boost converter. It is possible to conclude that the system is able to produce the same power for different load conditions with good dynamics.

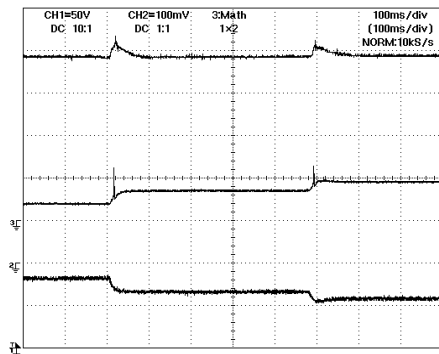


Fig. 10. Experimental result in mode II (MPPT test mode). Output voltage (CH1), output voltage (CH2) and output power (Ch3) considering two step load variations.

VII. CONCLUSIONS

This paper presents the development of a solar PV simulator system based on three buck-boost DC-DC power converters using a sliding mode controller in two of them. The solution can perform automatic test in two different modes to simulate the I-V characteristic curve of a solar PV panel and the MPPT algorithm adopted, which can be selected in a SCADA system as layout interface. The solution can be easily modified according to the values specified by manufactures. Experimental results have demonstrated the effectiveness and the good dynamic of the sliding mode controller applied to the system. Furthermore, experimental results demonstrate that the PV simulator can mimic a real solar PV panel in terms of solar irradiation and temperature variation. Also, the classic MPPT perturb and observe (P&O) algorithm is compatible with the operation cycle of a PLC, generating good results. The main limitation of the proposed solution is the available power circuits of the DC-DC converters (up to 350W) and the inability to run more complex MPPT algorithms. Other topologies should be adopted and tested in future works using a similar strategy to extend the operation of the proposed solution.

ACKNOWLEDGMENT

This work was supported by Instituto Politécnico de Lisboa, reference code: IPL/2021/ATS2SPV_ISEL.

REFERENCES

- [1] Renewables 2021 Global Status Report – a comprehensive annual overview of the state of renewable energy, REN21. <https://ren21.net/gsr-2021/>
- [2] S. Sousa, M. Onofre, T. Antunes, C. Branco, J. Maia, J. I. Rocha, V. Fernão Pires, "Implementation of a low-cost data acquisition board for photovoltaic arrays analysis and diagnostic", *Int. Conf. on Renewable Energy Res. and Appl. (ICRERA)*, pp. 1084-1088, October 20-23, 2013.
- [3] Y. Hishikawa et al., "Voltage-Dependent Temperature Coefficient of the I-V Curves of Crystalline Silicon Photovoltaic Modules," in *IEEE Journal of Photovoltaics*, vol. 8, no. 1, pp. 48-53, Jan. 2018.
- [4] M. Ünlü and S. Çamur, "A simple Photovoltaic simulator based on a one-diode equivalent circuit model," *2017 4th Int. Conference on Electrical and Electronic Engineering (ICEEE)*, pp. 33-36, 2017.
- [5] S.M. Hassan Hosseini, A.A. Keymanesh, "Design and construction of photovoltaic simulator based on dual-diode model," *Solar Energy*, Vol. 137, pp. 594-607, 2016.
- [6] M. S. Khalid, M.A. Abido, "A novel and accurate photovoltaic simulator based on seven-parameter model," *Electric Power Systems Research*, vol. 116, pp. 243-251, 2014.
- [7] S. Mann, E. Fadel, S. S. Schoenholz, E. D. Cubuk, S. G. Johnson, G. Romano, "oPV: An end-to-end differentiable solar-cell simulator," *Computer Physics Communications*, vol. 272, 108232, 2022.
- [8] C. Roncero-Clemente, E. Romero-Cadaval, V. M. Minambres, M. A. Guerrero-Martinez, J. Gallardo-Lozano, "PV Array Emulator for Testing Commercial PV Inverters," *Elektronika Ir Elektrotehnika*, 19(10), pp. 71-75, 2013.
- [9] L. Bun, B. Raison, G. Rostaing, S. Bacha, A. Rumeau and A. Labonne, "Development of a real time photovoltaic simulator in normal and abnormal operations," *IECON 2011 - 37th Annual Conference of the IEEE Industrial Electronics Society*, pp. 867-872, 2011.
- [10] N. Kahoul, M. Houabes, A. Neçaibia, "A comprehensive simulator for assessing the reliability of a photovoltaic panel peak power tracking system," *Front. Energy*, vol. 9 (2), Higher Education Press and Springer-Verlag Berlin Heidelberg, 2015, pp.170-179.
- [11] W. Subsingha, "Real-time Photovoltaic Simulator Using Current Feedback Control," *Energy Procedia*, vol. 89, pp. 160-169, 2016.
- [12] R. V. Parupudi, H. Singh, M. Kolokotroni, "Sun Simulator for Indoor Performance assessment of Solar Photovoltaic Cells," *Energy Procedia*, vol. 161, pp. 376-384, 2019.
- [13] U. K. Shinde, S. G. Kadwane, R. K. Keshri and S. P. Gawande, "Dual Mode Controller-Based Solar Photovoltaic Simulator for True PV Characteristics," in *Canadian Journal of Electrical and Computer Engineering*, vol. 40, no. 3, pp. 237-245, 2017.
- [14] W. Zhang and J. W. Kimball, "DC-DC Converter Based Photovoltaic Simulator with a Double Current Mode Controller," in *IEEE Trans. Power Elect.s.*, vol. 33, no. 7, pp. 5860-5868, July 2018.
- [15] D. Ghaderi, G. A. Bayrak, "Novel Step-Up Power Converter Configuration for Solar Energy Application." *Elektronika Ir Elektrotehnika*, 25(3), pp. 50-55, 2019.
- [16] A. Cordeiro, D. Foito and V. Fernão Pires, "A PV panel simulator based on a two quadrant DC/DC power converter with a sliding mode controller," *2015 International Conference on Renewable Energy Research and Applications (ICRERA)*, pp. 928-932, 2015.
- [17] H. Qi, Y. Bi and Y. Wu, "Development of a photovoltaic array simulator based on buck converter," *2014 Int. Conf. on Information Science, Electronics and Electrical Engineering*, pp. 14-17, 2014.
- [18] D. Lu, Q. Nguyen, "A photovoltaic panel emulator using a buck-boost DC/DC converter and a low-cost micro-controller," *Elsevier – Solar Energy*, vol. 86, 2012, pp.1477-1484.
- [19] R. Ahmad, A. F. Murtaza, and H. A. Sher, "Power tracking techniques for efficient operation of photovoltaic array in solar applications- A review," *Renewable and Sustainable Energy Reviews*, vol. 101, pp. 82-102, Mar. 2019.
- [20] M. A. G. de Brito, L. Galotto, L. P. Sampaio, G. D. A. e Melo, and C. A. Canesin, "Evaluation of the main MPPT techniques for photovoltaic applications," in *IEEE Transactions on Industrial Electronics*, vol. 60, no. 3, pp. 1156-1167, Mar. 2013.
- [21] R. B. Bollipo, S. Mikkili and P. K. Bonthagorla, "Hybrid, optimal, intelligent and classical PV MPPT techniques: A review," in *CSEE Journal of Power and Energy Systems*, vol. 7, no. 1, pp. 9-33, Jan. 2021.
- [22] Kuang-Hui Tang, Kuei-Hsiang Chao, Yuan-Wei Chao, Jyun-Ping Chen, "Design and Implementation of a Simulator for Photovoltaic Modules", *International Journal of Photoenergy*, vol. 2012, Article ID 368931, 6 pages, 2012.
- [23] W. Gao, J. Hung, "Variable structure control of nonlinear systems: a new approach", *IEEE Trans. Ind. Elect.*, vol. 40, no. 1, pp.45-55, 1993.
- [24] J. Fernando Silva, Sónia Ferreira Pinto, Advanced Control of Switching Power Converters, in Muhammad Rashid et al, ed: *Power Electronics Handbook 3ed*, Butter. Hein., 2011, chap. 36, pp. 1037-1114.
- [25] V. F. Pires, J. F. Martins, Chen Hao, "Dual-Inverter for Grid Connected Photovoltaic System: Modelling and Sliding Mode Control," *Solar Energy*, vol. 86, no. 7, pp. 2106-2115, 2012.
- [26] J. Mérida, L. T. Aguilar, J. Dávila, "Analysis and synthesis of sliding mode control for large scale variable speed wind turbine for power optimization", *Renewable Energy*, vol. 71, pp. 715-728, 2014.
- [27] <https://www.sungoldsolar.com/SGP-320W36V-Poly-Solar-Panel-pd6089854.html>.